Beam-Switch Wide-Swath Mode for Interferometrically Compatible Single-Pol and Quad-Pol SAR Products

Federica Bordoni, Paco López-Dekker, *Senior Member, IEEE*, and Gerhard Krieger, *Fellow, IEEE*

***Abstract*— Future spaceborne synthetic aperture radar (SAR) systems are expected to deliver enormous quantity of data. Accordingly, the observation plan becomes crucial for a proper allocation of the mission resources. A central challenge is to reduce the number of acquisitions by making the same image available for more applications. Here, a relevant restriction is the interferometric incompatibility between fully polarimetric (QP) and single polarimetric (SP) SAR images, which typically occurs when the acquisitions are performed in burst mode, as in case of SAR products with wide coverage acquired by means of ScanSAR or terrain observation by progressive scanning (TOPS) technique. In order to overcome this limitation, a new operational mode, denoted as beam-switch wide-swath (BSWS), was conceived. The BSWS mode exploits the operational flexibility of future SAR systems to generate SP images, interferometrically compatible with the QP ones, keeping the wide coverage characteristic of the SP products. This letter presents in detail the BSWS mode, analyzing its functional principle, and imaging performance, based on a realistic future SAR system, the high-resolution wide-swath (HRWS) SAR, considered for the next generation of the Sentinel-1 mission.**

***Index Terms*— Digital beamforming (DBF), high-resolution wide-swath (HRWS), interferometry, multichannel synthetic aperture radar (SAR).**

I. Introduction

FUTURE spaceborne synthetic aperture radar (SAR) will be able to deliver images with improved resolution, coverage, and quality if compared to the present systems. In particular, wide coverage and high resolution will be available at the same time [1]–[8]. As this new capability implies a tremendously increased data rate, a proper allocation of resources, such as on-board memory, downlink capacity, and orbit usage becomes crucial. In particular, the observation plan should be carefully defined to match the system capability with the SAR imaging requirements imposed by the end user [9].

A central challenge of the observation plan is to minimize the number of acquisitions by making the same image available for more applications [9]. Indeed, different applications impose different requirements on the acquisition. For instance, land cover monitoring requires full polarimetry (QP); whereas land deformation prefers single polarimetry (SP), since the priority is on the wide coverage, which is reduced in QP [8]–[10]. In this context, a relevant restriction is represented by the interferometric incompatibility between QP and SP images, when the acquisitions are performed in burst mode, as in case of wide swath SAR products acquired by means of ScanSAR or terrain observation by progressive scanning (TOPS) technique.

The interferometric compatibility between two SAR images requires common spectral components for each represented target. Since operating in burst mode leads to a space-variant azimuth spectrum, a synchronization of the burst timeline becomes necessary [11], [12]. Specifically, burst length and imaging geometry should be the same. Nevertheless, SP and QP acquisitions are generally characterized by completely different geometrical and timing parameters. In fact, in most cases, QP products are obtained by using a pulse repetition frequency (PRF) about twice than that in SP, as the polarization is toggled on transmission. Moreover, the swath extension in QP is reduced with respect to SP, due to the more severe timing and range-ambiguity constraints. Obviously, the trivial option of ensuring the compatibility by using the QP geometrical/timing parameters also for SP would result in an inacceptable reduced coverage of the SP images.

In order to deliver SP products that are interferometrically compatible with the QP products, while keeping the SP large coverage, a new operational mode, denoted as beam-switch wide-swath (BSWS), has been developed by the German Aerospace Center (DLR). This new mode was proposed within a recent European Space Agency (ESA) study focused on the high-resolution wide-swath (HRWS) system [4], which is a multichannel SAR with digital beamforming (DBF) capability, considered as preferential candidate for the next generation (NG) of Sentinel-1 (S-1) [8], [13].

Manuscript received January 15, 2018; revised May 9, 2018; accepted June 15, 2018. This work was supported by the European Space Agency (ESA) under ESA-ESTEC Contract 4000109920/14/NL/AT. *(Corresponding author: Federica Bordoni.)*

F. Bordoni and G. Krieger are with the Microwaves and Radar Institute, German Aerospace Centre, 82234 Wessling, Germany (e-mail: Federica.Bordoni@dlr.de; gerhard.krieger@dlr.de).

F. López-Dekker is with the Geoscience and Remote Sensing Department, Delft University of Technology, 2628 CN Delft, The Netherlands (e-mail: F.LopezDekker@tudelft.nl).

Color versions of one or more of the figures in this letter are available online at http://ieeexplore.ieee.org.

Digital Object Identifier 10.1109/LGRS.2018.2849269

TABLE I
HRWS SAR SYSTEM REFERENCE PARAMETERS

Quantity	Value
Orbit Height	700 km
Antenna Tilt Angle	31 deg
Pulse Repetition Frequency (PRF)	1200 - 2600 Hz
RF Centre Frequency	5.405 GHz
Available Radar Signal Bandwidth	150 MHz
Average Tx Power	900 W
Tx/Rx Antenna Size (Height x Length)	1.18 m x 12.8 m
Nr. of Digital Rx Chan. (Eleva. x Azi.)	7 x 8

First results, published within a conference paper, demonstrated the potentiality of the BSWS [14]. This letter reviews and deepens the analysis on the BSWS. The BSWS concept is explained exhaustively. The impact of this new operational mode on the SAR imaging performance computation is analyzed and the achievable SAR imaging performance investigated in detail. Moreover, possible solutions for improved SAR imaging performance are presented. The applicability of the BSWS mode to future SAR systems, different from the HRWS, is also discussed.

This letter is organized as follows. Section II describes the HRWS SAR system, used as a reference for the explanation of the BSWS concept in Section III, and for the performance analysis in Section IV. Conclusions are drawn in Section V.

II. REFERENCE SAR SYSTEM

The reference SAR system resembles the ESA HRWS system considered as baseline for the S-1 NG mission [6]–[8]. Its main parameters are reported in Table I. It is a C-band system orbiting at a height of 700 km. The architecture is based on a planar phased array antenna, 1.18 m high and 12.8 m long. On transmission (Tx), the phase spoiling (PS) technique is used to broaden the azimuth beam, in order to increase the Doppler bandwidth, whereas for the elevation beams both PS and amplitude taper are eventually used, according to the extension of the imaged surface. On receive (Rx), multiple digital Rx channels, uniformly distributed along the azimuth and range direction, are used in conjunction with DBF techniques to relax the constraints related with the high-resolution and wide-swath imaging. Specifically, eight azimuth channels are combined according to the azimuth multichannel reconstruction approach (MAPS) [1] and seven elevation channels implement the scan-on-receive (SCORE) [4].

The system has full polarimetric capability. In particular, for the QP products, the transmitted linear polarization is toggled from pulse to pulse; whereas for single- and dual-polarimetric (DP) products a single linear polarization is transmitted. On Rx, two simultaneous receivers are available, each dedicated to a specific linear polarization. Accordingly, SP and DP products could be assumed to have the same imaging performance. (The dependence of pattern shape and backscatter coefficient on polarization is neglected.)

III. BEAM-SWITCH WIDE-SWATH MODE

The HRWS system is expected to deliver SAR images with large coverage by operating in wide-swath (WS) mode,

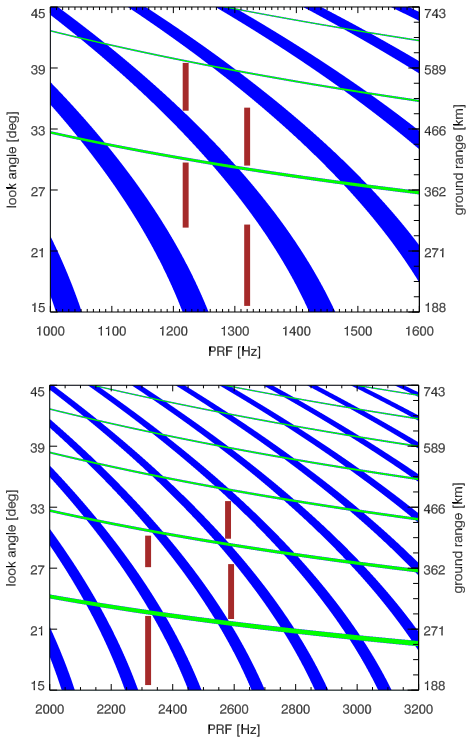

Fig. 1. Timing diagrams for the WS SP and DP (top) and WS QP (bottom) mode: the vertical segments denote the subswath locations (each associated with a PRF value and a spatial position); the white stripes denote the areas where signal reception is possible; the colored stripes denote blind areas associated with the Tx-event (blue lines) and the nadir echo (green lines).

according to the ScanSAR technique. The timing diagrams considered for the SP/DP and QP acquisitions in WS mode are shown in Fig. 1 (top and bottom, respectively). In both cases, the imaged swath is composed by four subswaths and is imaged in a single pass by using four bursts. Nevertheless, in WS SP/DP mode, the imaged swath reaches an extension of 400 km, whereas in WS QP mode, it covers just the 280 km located in near range. This geometrical relationship between the swaths imaged in SP/DP and in QP is typical. In fact, it is originated by the about twice higher PRF value used in QP and the related range-ambiguity constraints on the image quality.

Due to the different timing parameters, the WS SP/DP and WS QP products are interferometrically incompatible with respect to each other. In order to understand how the BSWS mode overcomes this limitation, it is useful to look at the BSWS timing diagram, shown in Fig. 2. The imaged swath has an extension of about 450 km and is covered by eight subswaths. The first four subswaths from near range are located exactly as in the WS QP mode (same PRF and same geometry). The other four are coupled with the previous ones: from near range, first with fifth, second with sixth, third with seventh, and fourth with eighth. Specifically, in the timing diagram, two coupled subswaths are located along the same vertical line and over regions (white stripes in Fig. 2) separated by two Tx-event blind regions (blue stripes). This means that they are associated with the same PRF value and with ground ranges, whose two-way time delays satisfy the

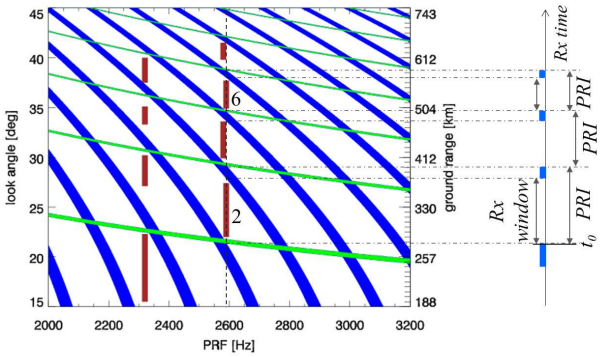

Fig. 2. Timing diagram for the BSWS mode. The relationship between two coupled subswaths (second and sixth) is evidenced on the left.

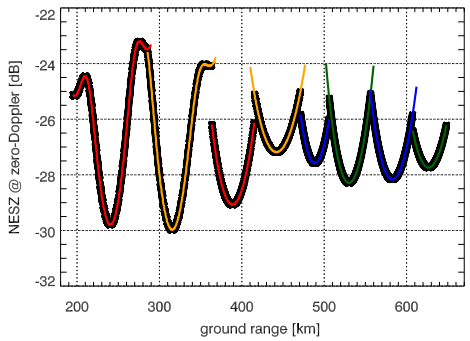

Fig. 3. NESZ computed at zero Doppler versus ground range.

following relationship (see Fig. 2):

$$t_0 < \tau < t_0 + \mathrm{PRI} \tag{1}$$

$$t_0 + 2\,\mathrm{PRI} < \tau_c < t_0 + 3\,\mathrm{PRI} \tag{2}$$

where PRI denotes the pulse repetition interval, τ is the two-way time delay of the near range subswath, t_0 is the minimum two-way time delay of the related Rx-window, and τ_c is the two-way time delay of the corresponding coupled subswath. It is worth remarking that such a subswath collocation is generally attainable, due to the mentioned geometrical relationship between the swaths imaged in SP/DP and QP, and to the (about twice) closer distribution of the Tx-event blind stripes in QP w.r.t. those in SP/DP (see Fig. 1).

All the eight subswaths are imaged within the same pass, in burst mode, by using four bursts. The two coupled subswaths are imaged during the same burst. This is achieved by exploiting the high PRF in a completely original way. Specifically, differently from the WS QP mode, in BSWS the transmitted polarization is constant, and the HRWS flexibility is used to switch the elevation Tx beam from pulse to pulse, so that the coupled subswaths are illuminated alternatively. Accordingly, a delay of PRI elapses between the transmission of the two subsequent pulses used to illuminate the coupled subswaths. Due to this delay and the location of the coupled subswaths [see (1) and (2)] the echoes from each of the coupled subswaths belong to different Rx-windows. Then, on Rx, a single SCORE beam allows recovering the echoes backscattered from the two coupled subswaths, by scanning them alternatively from Rx-window to Rx-window. The so recorded echoes from two subsequent pulses (within the same burst) are elaborated separately: each one is used to image one of the coupled subswaths, according to the conventional SAR processing, with a PRF half of the transmitted one.

The burst duration is chosen as in WS QP mode. Moreover, the chirp bandwidth, used to image the four near range subswaths, is set as for the WS QP acquisition. Accordingly, the SAR image of the first four subswaths obtained in BSWS and the WS QP image share the same spectral components and are interferometrically compatible.

IV. SAR Imaging Performance

As shown in Fig. 2, the swath extension in BSWS mode is about 450 km. The spatial resolution is about 5 m $\times$ 5 m in the first four subswaths in near range, as in the WS QP mode, due to the mentioned choice of the chirp bandwidth and burst duration. In the other four (coupled) subswaths, the azimuth resolution deteriorates, reaching a worst value of about 5.8 m. The difference in the azimuth resolution performance between the coupled subswaths is related to the BSWS operational mode. In fact, the illumination time is the same for the two coupled subswaths and is set taking into account only the near range geometry.

As regards the ground range resolution, it is assumed that the chirp bandwidth does not change between the coupled subswaths. Accordingly, in the four far range subswaths the ground range resolution is below 4 m, and the 2-D spatial resolution remains below 25 m^2 over the complete image. Another option would be to adapt the chirp bandwidth to the illuminated subswath from pulse to pulse, in order to have 5 m range resolution over the whole access range.

Besides spatial resolution and swath extension, the basic SAR image quality parameters are the noise equivalent sigma zero (NESZ), the range ambiguity-to-signal ratio (RASR), and the azimuth ambiguity-to-signal ratio (AASR). A compliant SAR imaging quality implies that the values of these parameters remain below a given threshold all over the image. In the considered case of the HRWS as S-1 NG, the threshold for both the NESZ and the total (range plus azimuth) ambiguity-to-signal ratio (ASR) is -22 dB.

Fig. 3 shows the NESZ computed at zero Doppler versus the ground range distance. The variation within each subswath is mainly induced by the elevation Tx beam shape. In particular, the Tx elevation patterns for the four near range subswaths are broadened by using the PS technique or an amplitude taper, whereas the others are uniformly weighted. In the four near range subswaths, the NESZ performance is exactly as in WS QP (assuming that the same patterns are used); in the far range subswaths, it has approximately the same mean level, since the uniform patterns have a higher gain than the broadened patterns, compensating the power attenuation induced by the geometry and by the smaller range resolution in far range. The NESZ performance additionally includes the scalloping, i.e., the signal power fluctuation induced by the burst operation. The obtained results show that this produces a maximum radiometric loss of about 1 dB versus the azimuth frequency. Thus, over the entire image, the NESZ remains below -22.2 dB, satisfying the mission requirements.

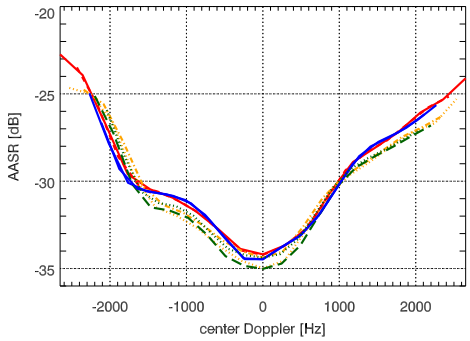

Fig. 4. AASR performance versus azimuth frequency.

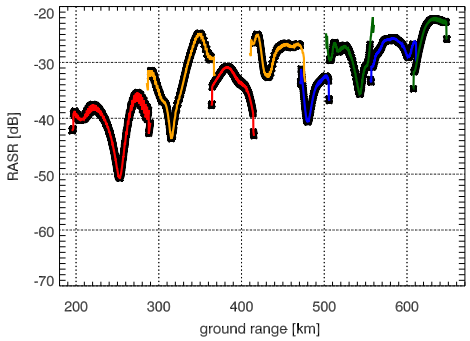

Fig. 6. RASR performance versus ground range.

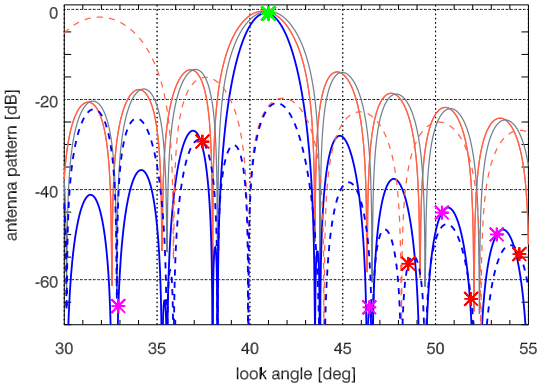

Fig. 5. Elevation patterns involved in the imaging of the eighth subswath (solid lines: patterns related with the imaged subswath; dashed lines: with the coupled subswath; orange lines: Tx, gray lines: Rx, and blue lines: two way). The position of the useful signal and ambiguous signals are marked by an asterisk (green: signal and red/magenta: ambiguities of odd/even order).

Fig. 4 shows the AASR versus the azimuth frequency. It reaches the worst value at the highest frequencies: −22.8 dB for the four near range subswaths and −24.7 dB for the coupled, far range subswaths. The difference in the AASR performance between the coupled subswaths is related to the mentioned setting of the illumination time in BSWS mode.

The BSWS operational mode affects also the computation of the RASR. In fact, as shown in Fig. 5, due to the Tx beam switch from pulse to pulse, the range ambiguities are weighted by different Tx elevation patterns: the ambiguities of even order are weighted, as the useful signal, by the Tx pattern illuminating the subswath of interest; those of odd order by the Tx pattern illuminating the subswath coupled with the subswath of interest.

The RASR performance versus the ground range is shown in Fig. 6. It remains below −24.5 dB in the first five subswaths from near range, whereas in the other subswaths it remains below −21.5 dB, with a worst value reached in the eighth subswath. This result does not allow fulfilling the specified requirements on the ASR of −22 dB. In fact, taking into account the achieved AASR, the RASR should be below about −30 dB in the four near range subswaths and −25.5 dB in far range.

It is worth pointing out that the RASR performance is affected by a degradation inherent to the BSWS mode. In fact, as mentioned, in BSWS mode, the range ambiguous returns of odd order arise from pulses illuminating the subswath coupled with the imaged one. Since these returns are weighted by the Tx elevation pattern illuminating the coupled subswath, they could be associated with a relevant power. Particularly critical are the ambiguities of first order, which are weighted by the main sidelobes of the Rx pattern. Moreover, the ambiguous returns from near range experience the power amplification induced by the backscatter coefficient and the geometry.

In order to mitigate the RASR performance degradation induced by the pulses directed to the coupled subswath, different techniques can be employed. An option with a limited impact on the instrument complexity is to use an amplitude taper, to reduce the sidelobe level of the Rx elevation pattern, at the cost of the radiometric performance. For instance, by using a Hamming taper, with a degradation of 1 dB on the NESZ, it is possible to achieve an RASR below −25.2 dB in near and −25.5 dB in far range. Though this performance does not meet the mission requirements on the image quality, it suggests that a minor change in the system configuration would be sufficient.

Alternatively, if not possible, in order to achieve a complete suppression of the ambiguous interference, orthogonal pulses can be employed to illuminate the coupled subswaths. Particularly, appealing for its limited impact on the system complexity is the multi-frequency (MF) approach [15]. According to it, pulses with disjoint bandwidths are transmitted and the corresponding echoes are separated on Rx by bandpass filters. For the present design, the separation could be completely done on ground, since the useful echoes belong to different Rx-windows. Moreover, since the first and fifth subswaths already reach a satisfactory performance (see Fig. 6), the MF approach could be simply applied to the other six subswaths. For these subswaths, the considered chirp bandwidth varies between about 74 and 55 MHz, so that the HRWS available radar signal bandwidth of 150 MHz would be enough for applying the MF. More in general, the obtainability of a wider radar signal bandwidth should not be a technological issue, and for other future SAR systems it is already planned. The RASR performance, obtained in BSWS mode by recurring to the MF approach, is shown in Fig. 7: over the complete imaged swath the RASR remains below the −32 dB, ensuring a compliant image quality.

It is worth pointing out that a limited number (one or two) of dominant ambiguous echoes are responsible for the poor

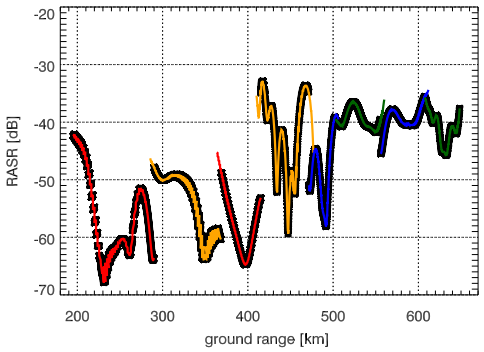

Fig. 7. RASR performance improved by the MF approach.

RASR result, and that these echoes are never weighted by the mainlobe of the Rx pattern. Under these conditions, an approach for pattern shaping, based on the minimum variance distortionless response with sidelobe constraints [16], [17], could be applied. According to it, the DBF capability of the system is exploited to design an Rx pattern with low levels in correspondence of the expected direction of arrival of the dominant ambiguities, without degradation of the imaging radiometric performance [16]. In the present case, under the realistic assumption that the dominant ambiguous returns would be attenuated by -10 dB, the mission requirements on the RASR performance and the overall image quality would be fulfilled.

The presented analysis suggests that SAR systems, designed to achieve satisfactory imaging performance in SP and QP burst modes, could properly operate also in BSWS mode. It must be remarked that the BSWS mode is presented here by considering a multichannel system with DBF capability (SCORE and MAPS). Nevertheless, even if DBF techniques allow for improved imaging performance, they are not necessary for using the BSWS mode: the basic prerequisite is just the possibility to switch the Tx beam from pulse to pulse. Accordingly, the BSWS mode can be applied also to simpler SAR systems without DBF capability, especially in conjunction with the MF approach.

V. Conclusion

A novel operational mode, the BSWS, was recently proposed by DLR in the frame of an ESA study on the HRWS SAR system, candidate for the next generation of the Sentinel-1 mission. The BSWS mode exploits in an original way the system operational flexibility, to generate single-pol images interferometrically compatible with the quad-pol ones, while keeping the wide coverage typical of the single-pol products.

With reference to the HRWS SAR system, the BSWS concept was explained and the SAR imaging performance analyzed in detail, showing how interferometrically compatible products with a coverage of 450 km can be obtained. Moreover, the compliance of the SAR imaging performance with the mission requirements was discussed, identifying possible BSWS limitations and proposing solutions. The obtained results demonstrate the possibility to achieve high image quality and suggest a successful employment of the BSWS mode in the future SAR systems.

Acknowledgment

The authors would like to thank their colleague F. Q. de Almeida for the useful discussion and the technical support.

References

[1] G. Krieger, N. Gebert, and A. Moreira, "Unambiguous SAR signal reconstruction from nonuniform displaced phase center sampling," *IEEE Trans. Geosci. Remote Sens. Lett.*, vol. 1, no. 4, pp. 260–264, Oct. 2004.

[2] N. Gebert, G. Krieger, and A. Moreira, "Digital beamforming on receive: Techniques and optimization strategies for high-resolution wide-swath SAR imaging," *IEEE Trans. Aerosp. Electron. Syst.*, vol. 45, no. 2, pp. 564–592, Apr. 2009.

[3] I. Sikaneta, C. H. Gierull, and D. Cerutti-Maori, "Optimum signal processing for multichannel SAR: With application to high-resolution wide-swath imaging," *IEEE Trans. Geosci. Remote Sens.*, vol. 52, no. 10, pp. 6095–6109, Oct. 2014.

[4] M. Suess, B. Grafmueller, and R. Zahn, "A novel high resolution, wide swath SAR system," in *Proc. IEEE IGARSS*, Sydney, NSW, Australia, vol. 3, Jul. 2001, pp. 1013–1015.

[5] F. Bordoni, M. Younis, and G. Krieger, "Performance investigation on the high-resolution wide-swath SAR system operating in stripmap quad-pol and ultra-wide ScanSAR mode," in *Proc. IEEE IGARSS*, Vancouver, BC, Canada, Jul. 2011, pp. 4469–4472.

[6] G. Adamiuk, C. Schaefer, C. Fischer, and C. Heer, "SAR architectures based on DBF for C- and X-band applications," in *Proc. EUSAR*, Berlin, Germany, Jun. 2014, pp. 16–19.

[7] M. Ludwig, M. Suess, N. Ayllon, and G. Adamiuk, "Digital beam forming for C-band SAR and technological elements," in *Proc. IGARSS*, Milan, Italy, Jul. 2015, pp. 192–195.

[8] M. J. Sanjuan-Ferrer *et al.*, "High resolution wide swath SAR applications study: An overview," in *Proc. ARSI KEO*, Noordwijk, The Netherlands, Nov. 2014, pp. 1–8.

[9] D. B. Tridon *et al.*, "Tandem-L observation concept—Contributions and challenges of systematic monitoring of earth system dynamics," in *Proc. IRS*, Prague, Czech Republic, Jun. 2017, pp. 1–9.

[10] Z. Malenovský *et al.* "Sentinels for science: Potential of Sentinel-1, -2, and -3 missions for scientific observations of ocean, cryosphere, and land," *Remote Sens. Environ.*, vol. 120, pp. 91–101, May 2012.

[11] A. M. Guarnieri and C. Prati, "ScanSAR focusing and interferometry," *IEEE Trans. Geosci. Remote Sens.*, vol. 34, no. 4, pp. 1029–1038, Jul. 1996.

[12] P. Prats-Iraola, R. Scheiber, L. Marotti, S. Wollstadt, and A. Reigber, "TOPS interferometry with TerraSAR-X," *IEEE Trans. Geosci. Remote Sens.*, vol. 50, no. 8, pp. 3179–3188, Aug. 2012.

[13] P. Snoeij *et al.*, "The Sentinel-1 radar mission: Status and performance," in *Proc. RADAR*, Oct. 2009, pp. 1–6.

[14] F. Bordoni, F. López-Dekker, and M. J. Sanjuan-Ferrer, "Beam-switch wide swath mode for interferometrically compatible products of the post-sentinel HRWS SAR system," in *Proc. IRS*, Prague, Czech Republic, Jun. 2017, pp. 1–6.

[15] F. Bordoni, G. Krieger, and M. Younis, "Multi-frequency subpulse SAR: Exploiting chirp bandwidth for an increased coverage," *IEEE Trans. Geosci. Remote Sen. Letters*, to be published.

[16] J. Liu, A. B. Gershman, Z.-Q. Luo, and K. M. Wong, "Adaptive beamforming with sidelobe control: A second-order cone programming approach," *IEEE Signal Process. Lett.*, vol. 10, no. 11, pp. 331–334, Nov. 2003.

[17] F. Q. De Almeida, T. Rommel, M. Younis, G. Krieger, and A. Moreira, "Multichannel staggered SAR: System concepts with reflector and planar antennas," *IEEE Trans. Aerosp. Electron. Syst.*, to be published.